NOTICE: When government or other drawings, specifications or other data are used for any purpose other than in connection with a definitely related government procurement operation, the U. S. Government thereby incurs no responsibility, nor any obligation whatsoever; and the fact that the Government may have formulated, furnished, or in any way supplied the said drawings, specifications, or other data is not to be regarded by implication or otherwise as in any manner licensing the holder or any other person or corporation, or conveying any rights or permission to manufacture, use or sell any patented invention that may in any way be related thereto.

63-4-5

AEDC-TDR-63-155

THE ABSORPTANCE OF A WATER CRYODEPOSIT AT 77°K FOR 350°K RADIATION

By

T. M. Cunningham, Jr.
Aerospace Environmental Facility
ARO, Inc.
and
R. L. Young
Professor of Mechanical Engineering
The University of Tennessee

TECHNICAL DOCUMENTARY REPORT NO. AEDC-TDR-63-155

August 1963

Program Element 61405014/8951, Task 895107

(Prepared under Contract No. AF 40(600)-1000 by ARO, Inc.,
contract operator of AEDC, Arnold Air Force Station, Tenn.)

ARNOLD ENGINEERING DEVELOPMENT CENTER

AIR FORCE SYSTEMS COMMAND

UNITED STATES AIR FORCE

NOTICES

THE ABSORPTANCE OF A WATER CRYODEPOSIT AT 77°K FOR 350°K RADIATION

By

T. M. Cunningham, Jr.
Aerospace Environmental Facility
ARO, Inc.
a subsidiary of Sverdrup and Parcel, Inc.

and

R. L. Young
Professor of Mechanical Engineering
The University of Tennessee

August 1963

ARO Project No. SW2103

ABSTRACT

The results of an investigation to determine the effect of a water cryodeposit on the radiative properties of two surfaces are presented. The experimental apparatus consisted of a concentric-cylinder calorimeter in which the inner cylinder was a blackbody heater maintained at about 77°K. Data are presented for the total hemispherical absorptance versus the thickness of water frost formed on a vacuum-metallized aluminum surface and on a Parson's black surface. It was found that the absorptance of the cryodeposit-wall complex attained a value of about 0.95 for frost thicknesses on the order of 0.1 mm. For thicknesses greater than 0.1 mm, the absorptance of the complex was found to be independent of the nature of the wall surface in contrast to earlier results for carbon dioxide cryodeposits.

PUBLICATION REVIEW

This report has been reviewed and publication is approved.

Hans K. Doetsch
H. K. Doetsch
Technical Advisor
DCS/Research

D. R. Eastman, Jr.
Donald R. Eastman, Jr.
DCS/Research

CONTENTS

ILLUSTRATIONS

NOMENCLATURE

A	Area
d	Volumetric density
$\mathfrak{F}$	Radiant interchange factor
k	Absorption coefficient
m	Mass
q	Rate of heat transfer
T	Temperature
t	Cryodeposit thickness
X	Ratio
α	Absorptivity or absorptance
ϵ	Emissivity or emittance
μ	Microns (10^{-3} mm)
ρ	Reflectivity or reflectance
σ	Stefan-Boltzmann constant

SUBSCRIPTS

f	Frost
i	Inner
o	Outer
w	Wall

1.0 INTRODUCTION

In recent years, much research effort has been directed toward determining the thermal radiative properties of materials. The major stimulus for these investigations has arisen from the utilization of a great variety of new alloys, plastics, ceramics, and surface coatings in space applications. In the absence of a convective medium, thermal energy transfer must occur by radiation. To be able to evaluate or predict this transfer, the emittance, absorptance, and reflectance* of the vehicle's surface must be known.

In space simulation, thermal radiative properties become important for another reason. One of the parameters to be simulated in an environmental chamber is the heat sink of outer space which behaves as a blackbody at a temperature of about 4°K. Radiation emitted by and reflected from the vehicle to outer space does not return to the vehicle. But, in the environmental chamber, this radiation must interact with the chamber walls, which are for the most part cryopumping surfaces. It is possible to treat the cryosurface with some sort of high absorptance coating such as Parson's black to provide initially near blackbody conditions. However, because of the gradual accumulation of a cryodeposit on the walls, a high value of absorptance may not be maintained. Therefore, it is necessary to determine the effect of cryodeposit thickness on the absorptance of cryodeposit-wall complexes.

At liquid-nitrogen (LN_2) temperatures, two of the more common components of the cryodeposit will be carbon dioxide and water. A previous report by the authors (Ref. 1) dealt with the effect of a carbon dioxide cryodeposit on the absorptance of a number of substrates. It was found that the absorptance of the complex was a continuing function of the substrate absorptance. This observation was explained, in part, on the basis of transmission bands in the CO_2 spectrum. A similar investigation of the effect of a water cryodeposit on substrates of high and low absorptance is described in this report.

To measure the total hemispherical absorptance calorimetrically, the investigator may choose among several geometries for which the radiative interchange factor is well known: infinite parallel plates, infinite concentric cylinders, and concentric spheres (Ref. 2). An

---

*Reflectance equals one minus the absorptance for opaque substances.

Manuscript received July 1963.

approximation to the infinite cylinder geometry was chosen for this experiment because of the relative ease of construction and the fact that the test surface could be observed continuously during the test. By determining the rate of heat transfer between the cylinders, the equilibrium surface temperatures, the respective areas, and the emittance of one of the surfaces, the absorptance of the other surface was calculated.

2.0 APPARATUS AND PROCEDURE

The experimental apparatus consists essentially of two concentric cylinders. In the cutaway drawing (Fig. 1), the cylinders are shown in their test position. The inner cylinder is the blackbody heater, and the test surface is the inner surface of the outer cylinder. The heater support contains the gas injection system and is movable to allow the heater to be lowered from the test area during the frosting process (Fig. 2). The test surface is cooled by maintaining a constant flow of LN_2 through the annular space behind the test surface. A pressure of 1×10^{-7} torr or less is maintained in the vacuum chamber by a LN_2-baffled oil diffusion pump.

Several requirements were essential in the heater design: (1) all the electrical energy supplied to the heater at equilibrium should be transferred by radiation to the test surface; (2) the surface temperature should be uniform over the entire length of the heater; (3) the surface temperature should be accurately measured, and (4) the emittance of the heater surface should be known and should approach unity. To accomplish these requirements, the heater was constructed with three heating elements: a 12-inch main heater and a one-inch guard heater on either end. Each was supplied independently by a d-c power supply so that no induction losses would occur. By maintaining the temperature of the guard heaters at the same temperature as the main heater, axial conduction and radiation losses were minimized. Use of the guard heaters and care in winding the heaters resulted in an axial temperature difference of no more than $\pm 2°K$.

The outer surface of the heater was a thin wall, copper tube which fitted tightly over the heater windings. Copper-constantan thermocouples were brought through the interior of the heater, and their junctions were soldered to the copper tube to assure good thermal contact. By coating the outer surface of the heater with Parson's black lacquer ($\epsilon = 0.98$, Ref. 3), an approximate blackbody was obtained. The finished heater is shown in Fig. 3.

The test surface assembly consisted of the test surface proper, an annulus behind the test surface for the LN_2 coolant, and a vacuum jacket.

It was made slightly longer than the heater to better the approximation to an infinite cylinder. For low absorptance substrate tests, the inner surface was polished to a surface finish of 2 micro-inches RMS then coated with evaporated aluminum (Fig. 4). The absorptance of this surface was measured and found to have a value of 0.06. At the conclusion of the low absorptance tests, the surface was coated with Parson's black lacquer for the high absorptance runs (Fig. 5).

A line drawing of the gas injection system is shown in Fig. 6. External to the vacuum chamber, the system consists of a pressurized helium supply, a heating coil, a water container, and a valving arrangement which allows the helium to pass through the water container or to bypass it. A vacuum valve at the fill tube inlet permits the chamber to be evacuated after the injection process. These valves are shown in Fig. 7.

The fill tube runs inside the heater support. In the injection area, large holes are drilled in the fill tube. When the heater is lowered into the injection position, a section of the heater support having a number of small holes is brought into the test surface area (Fig. 8). The holes cover a section of the heater support roughly equivalent in length to the test surface. These holes backed by the larger holes in the fill tube provide a "diffuser" action which permits a uniform coverage of the test surface.

In a typical run, water was placed in the stainless steel container, and the mass of water injected was determined by weighing the container on an analytical balance before and after the injection. Heated helium gas flowed through the bypass valve and into the system until the temperature of all the gas injection system's components was high enough to prevent condensation of water in the injection system. Then the bypass valve was closed, and the helium bubbled through the water, carried water vapor into the chamber, and deposited it onto the test surface. During the injection, the heated helium was alternately passed through the water and bypassed through the system to prevent the accumulation of water in any of the lines. Throughout the injection process, the pressure in the chamber was approximately one torr.

Once the cryodeposit was in place, the heater was retracted into its normal position and the vacuum valve was closed. The vacuum chamber was then evacuated to the 10^{-7}-torr range where convective heat transfer is negligible. After some experience with the equipment, it was possible to adjust the power levels of the three heaters so that the equilibrium temperature was about 350°K. Equilibrium was determined by monitoring the heater temperature on a strip chart recorder. When no temperature change was observed in readings taken one hour apart, it was judged that equilibrium had been reached.

The power input to the heater was measured by a standard voltbox-shunt arrangement, and the equilibrium temperatures of three centrally located thermocouples were read with a potentiometer and averaged. These readings together with the respective areas of the test surface and the heater gave the data necessary to calculate the absorptance of the test surface.

3.0 METHODS OF CALCULATION

3.1 ABSORPTANCE

The equation

$$q_{io} = \sigma A_i \mathfrak{F}_{io} (T_i^4 - T_o^4) \qquad (1)$$

where

q_{io} = measured rate of radiation heat transfer between heater surface i and test surface o

σ = Stefan-Boltzmann constant, $\frac{\text{watts}}{\text{cm}^2 - °\text{K}^4}$

A_i = surface area of heater, cm^2

$\mathfrak{F}_{io}$ = radiant energy interchange factor between surface i and o

T_i = surface temperature of heater, °K

T_o = temperature of test surface, °K

can be used to calculate the rate of radiation heat transfer between bodies at different temperatures (Refs. 4 and 5). In this investigation, $T_i \approx 350°$ while $T_o \approx 77°K$.

Rewriting Eq. (1) as

$$q_{io} = \sigma A_i \mathfrak{F}_{io} T_i^4 \left[1 - \left(\frac{T_o}{T_i}\right)^4\right] \qquad (2)$$

but

$$\left(\frac{T_o}{T_i}\right)^4 \ll 1$$

Therefore

$$q_{io} = \sigma A_i \mathfrak{F}_{io} T_i^4 \qquad (3)$$

For infinite concentric cylinders, the radiative interchange factor is (Ref. 2)

$$\mathfrak{F}_{io} = \frac{1}{\frac{1}{\epsilon_i} + \left(\frac{1}{\alpha_o} - 1\right)\frac{A_i}{A_o}} \qquad (4)$$

where

ϵ_i = emissivity of heater surface

α_o = absorptance of test surface

A_o = area of the test surface, cm^2

Substituting Eq. (4) into Eq. (3) and solving for α_o gives

$$\alpha_o = \frac{1}{1 + \frac{A_o}{A_i}\left(\frac{A_i \sigma T_i^4}{q_{io}} - \frac{1}{\epsilon_i}\right)} \tag{5}$$

Equation 5 was used in calculating the results. While it is strictly valid for infinite concentric cylinders having diffusely reflecting gray body walls, a numerical approach to the problem, accounting for these deviations, yielded results differing by less than the experimental error.

3.2 FROST THICKNESS

Because the frost thickness could not be measured directly, it was necessary to calculate it from the mass of water injected, the area of the test surface, and the density of water.

$$t = \frac{0.1\ m}{A_o\ d} \tag{6}$$

where

t = thickness, mm

m = mass of water, g

A_o = test surface area, cm^2

d = volumetric density, g/cm^3

4.0 DATA AND RESULTS

The experimental data are presented as a plot of absorptance versus frost thickness for the evaporated aluminum and Parson's black substrates (Fig. 9). For the aluminized surface, a rapid increase in absorptance with frost thickness is observed for very thin deposits. At a thickness of 0. 1 mm, the absorptance attains a value of about 0. 95, and no further increase in absorptance is observed as this thickness increases to 0. 16 mm. The deposit on the Parson's black substrate causes the absorptance to decrease slightly to a value of about 0. 95 for a thickness of 0. 1 mm; essentially no change is observed thereafter although the frost thickness was increased to 0. 16 mm.

A comparison of these data with those previously reported for carbon dioxide cryodeposits (Ref. 1) shows that the carbon dioxide cryodeposit has much less effect on the complex absorptance than does the water cryodeposit. For example, a 0.20-mm-thick carbon dioxide cryodeposit on a highly reflecting substrate has an absorptance of only about 0.20. This difference can be explained if it is assumed that the value obtained for the water is characteristic only of the frost itself, whereas the absorptance value for the carbon dioxide continues to depend upon the absorptance of the substrate. The data in Ref. 1 indicate that the carbon dioxide cryodeposit transmits some wavelengths of the incident radiation without absorption, whereas the water cryodeposit tends to absorb all incident radiation. Spectral results for carbon dioxide in the solid state by Dahlke (Ref. 6) and for water in the solid state by Giguere and Harvey (Ref. 7) support these conclusions.

The following equation was used to represent the experimental data obtained for carbon dioxide cryodeposits (Ref. 1):

$$\rho_o = \rho_w + X\left(1 - e^{-kt}\right)(\rho_f - \rho_w) \tag{7}$$

where

ρ_o, ρ_f, ρ_w = reflectance of cryodeposit-wall complex, frost, and wall, respectively

X = ratio of the energy in absorbable wavelengths to the total incident energy

k = absorption coefficient, mm^{-1}

t = thickness, mm

Because the data indicate that there is no selective absorption in the water cryodeposit, X is taken as unity in Eq. (7), and absorptance is used in place of reflectance. Thus

$$a_o = a_f + e^{-kt}(a_w - a_f) \tag{8}$$

Evaluating α_f and k in Eq. (8) from the experimental data given

$$a_f = 0.95 \qquad k = 130 \text{ mm}^{-1}$$

The value for α_f was determined from the extrapolated value for α_o as the cryodeposit thickness approached infinity. The value of k was obtained from a least squares best fit method of all data. A value of k on the order of 50 mm^{-1} better fits the data for the evaporated aluminum surface, whereas a higher value of k better fits the data for the black surface.

The following equation provides a reasonable representation of the data shown in Fig. 9:

$$\alpha_o = 0.95 + e^{-130t}(\alpha_w - 0.95) \tag{9}$$

where t is the frost thickness in mm.

The observation that the water cryodeposit is a much stronger absorber of radiation than the carbon dioxide cryodeposit is illustrated by the values of k found for the two cases. For a carbon dioxide cryodeposit, $k = 4\ mm^{-1}$ (Ref. 1), whereas for the water cryodeposit, $k \approx 130\ mm^{-1}$.

5.0 DISCUSSION OF ERROR

5.1 ABSORPTANCE

The uncertainty interval (estimated error) in the experimental values for α_o can be determined by estimating the uncertainty intervals in each of the measured quantities used to calculate α_o by Eq. (5). Following the method of Ref. 8

$$\pm \Delta\alpha_o = \left[(\Delta A_o)^2 + (\Delta T_i)^2 + (\Delta q_{io})^2 + (\Delta A_i)^2 + (\Delta \epsilon_i)^2\right]^{1/2}$$

where $\pm\Delta\alpha_o$ = uncertainty interval in experimental value of α_o

$$\Delta A_o,\ \Delta T_i,\ \text{etc.} = \frac{\partial \alpha_o}{\partial A_o}\,\delta A_o,\ \frac{\partial \alpha_o}{\partial T_i}\,\delta T_i,\ \text{etc.}$$

The partial derivatives, $\frac{\partial \alpha_o}{\partial A_o}$, $\frac{\partial \alpha_o}{\partial T_i}$, are obtained from Eq. (5), and the uncertainty intervals in each measured quantity (δA_o, δT_i, etc.) are estimated as follows:

$A_o \pm \delta A_o$ = 998 cm^2 ±4 cm^2 (δA_o allows for change in area because of frost accumulation.)

$T_i \pm \delta T_i$ = 350°K ±2°K

$q_{io} \pm \delta q_{io}$ = 5 watts ±0.2 watt for α_o near zero
40 watts ±0.2 watt for α_o near unity

$A_i \pm \delta A_i$ = 718 cm^2 ±1 cm^2

$\epsilon_i \pm \delta \epsilon_i$ = 0.98 ±0.01

Using these values of estimated uncertainty intervals, the uncertainty interval in α_o is found to be

$$\Delta\alpha_o = \pm 0.003 \text{ for } \alpha_o \text{ near zero}$$

$$\Delta\alpha_o = \pm 0.04 \text{ for } \alpha_o \text{ near unity}$$

5.2 FROST THICKNESS

The greatest uncertainty in the calculation of frost thickness results from the lack of an accurate value for the density of water at 77°K. Even if such a number were available, the density may vary considerably with the manner in which the deposit is formed.

In the previous report on carbon dioxide, it was found that the density of the carbon dioxide cryodeposit decreased by a factor of 2 from the value reported for dry ice. There is some evidence that this is also true for the water cryodeposit, but the magnitude of the factor is yet to be determined. Hence, the value of 0.9168 (Ref. 9) was used with the understanding that it is strictly valid only for ice at 0°C and atmospheric pressure.

Because of the uncertainty in the value of density, the data are presented in terms of both frost thickness and "surface density." The "surface density" is the mass of water injected divided by the test surface area. Should accurate data become available on the density of water cryodeposits at this temperature, the frost thickness may then be determined by dividing the surface density by the volumetric density.

6.0 CONCLUSIONS

As a result of the study on the effect of a water cryodeposit on the radiative properties of two surfaces, it is concluded that

1. The addition of a water cryodeposit to a substrate rapidly changes the absorptance of the complex to a value near unity for 350°K radiation.
2. The absorptance of the substrate has no influence upon the complex absorptance for water frost thicknesses greater than 0.1 mm.
3. If the major outgassing or inleakage product in an environmental chamber is water, no special surface treatment will be required to obtain the desired high absorptance for infrared radiation on the cryogenically cooled wall surfaces.

REFERENCES

1. Cunningham, T. M., Jr., and Young, R. L. "The Radiative Properties of Carbon Dioxide Cryodeposits at 77°K." AEDC-TDR-62-165, December 1962.
2. Jakob, M. Heat Transfer. Vol. 2, John Wiley and Sons, Inc., New York, 1957.
3. MacDowall, J. "A Total Radiation Fluxmeter." Met. Res. Ctec., Air Ministry, London M.R.P. No. 858, 1954.
4. Zimmermann, F. J. "Total Emissivities and Absorptivities of Some Commercial Surfaces at Room and Liquid-Nitrogen Temperatures." Journal of Applied Physics, Vol. 26, No. 12, 1955, pp. 1483-1488.
5. Fulk, M. M., and Reynolds, M. M. "Emissivities of Metallic Surfaces at 77°K." Journal of Applied Physics, Vol. 28, No. 12, December 1957, pp. 1464-1467.
6. Dahlke, W. "Vibration Bands of Solid Carbon Dioxide." Z. Physik, Vol. 102, 1936, p. 360.
7. Giguere, P. A., and Harvey, K. B. "On the Infrared Absorption of Water and Heavy Water in Condensed States." Canadian Journal of Chemistry, Vol. 34, 1956, p. 798.
8. Kline, S. J., and McClintock, F. A. "Describing Uncertainties in Single Sample Experiments." Mechanical Engineering, Vol. 79, No. 1, January 1953, p. 3.
9. Hodgman, Charles D. (Editor) Handbook of Chemistry and Physics. Chemical Rubber Publishing Company, Cleveland, Ohio, 1962. (43rd Edition).

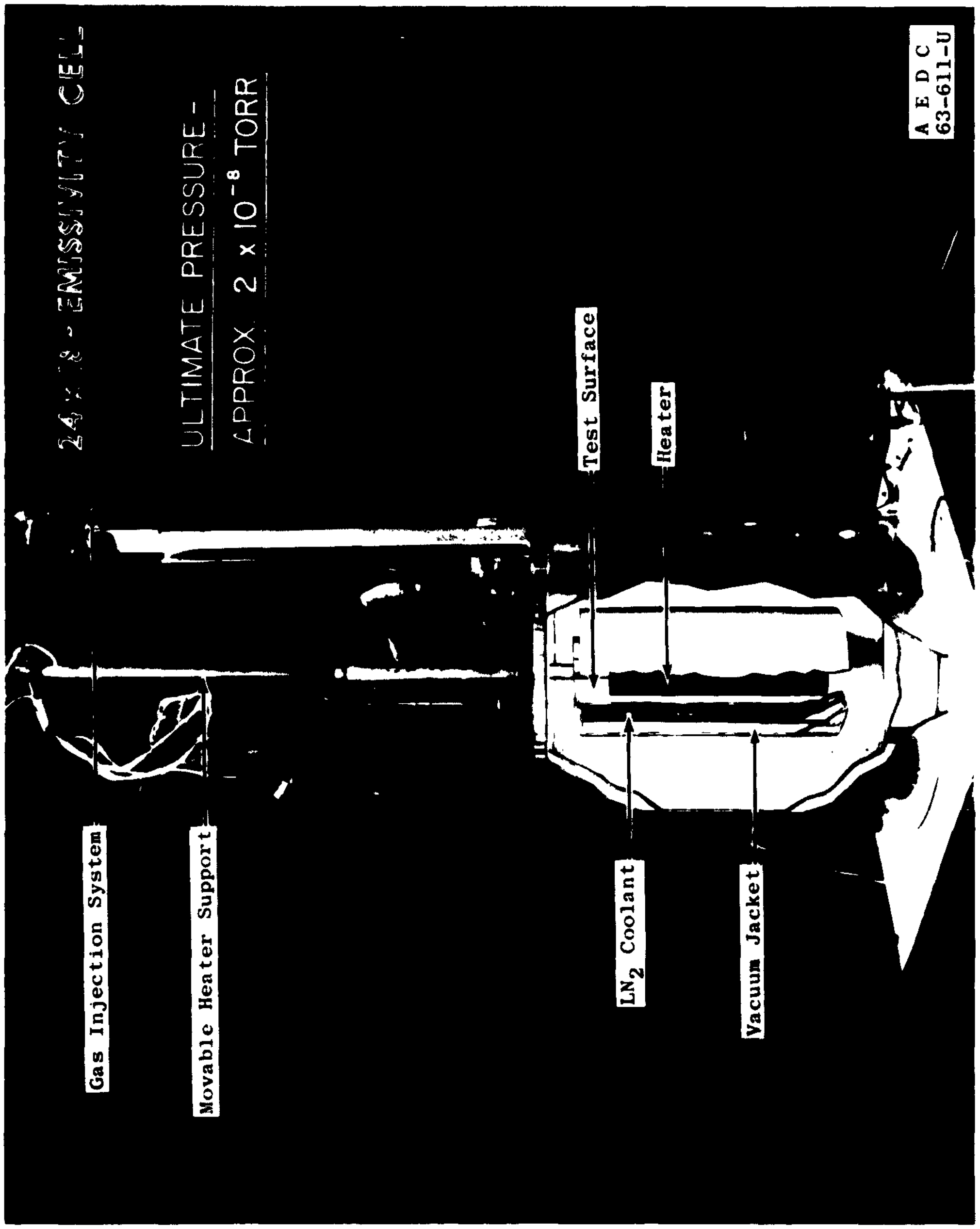

Fig. 1 Test Apparatus

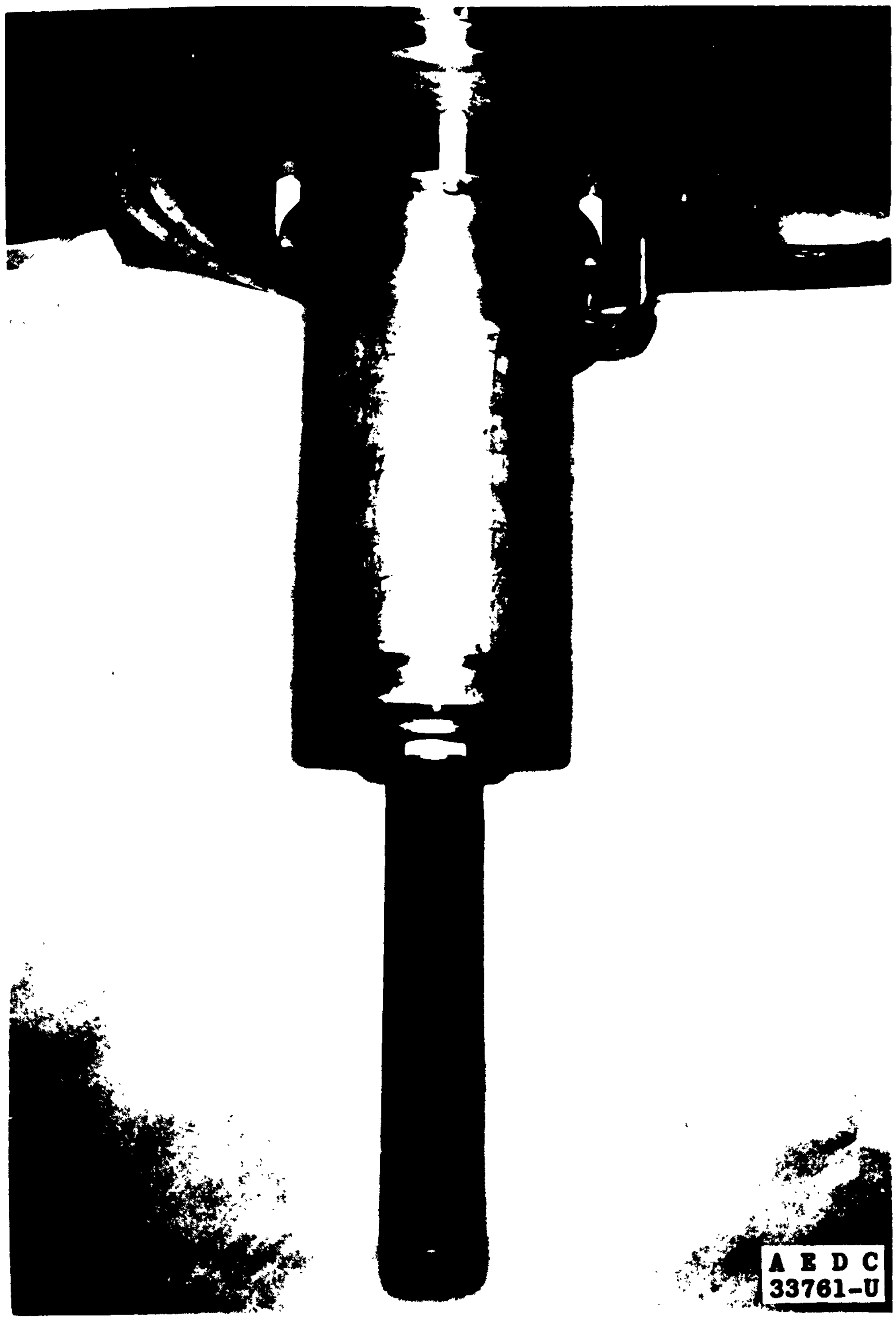

Fig. 2 Heater Extended from Cryoarray Assembly

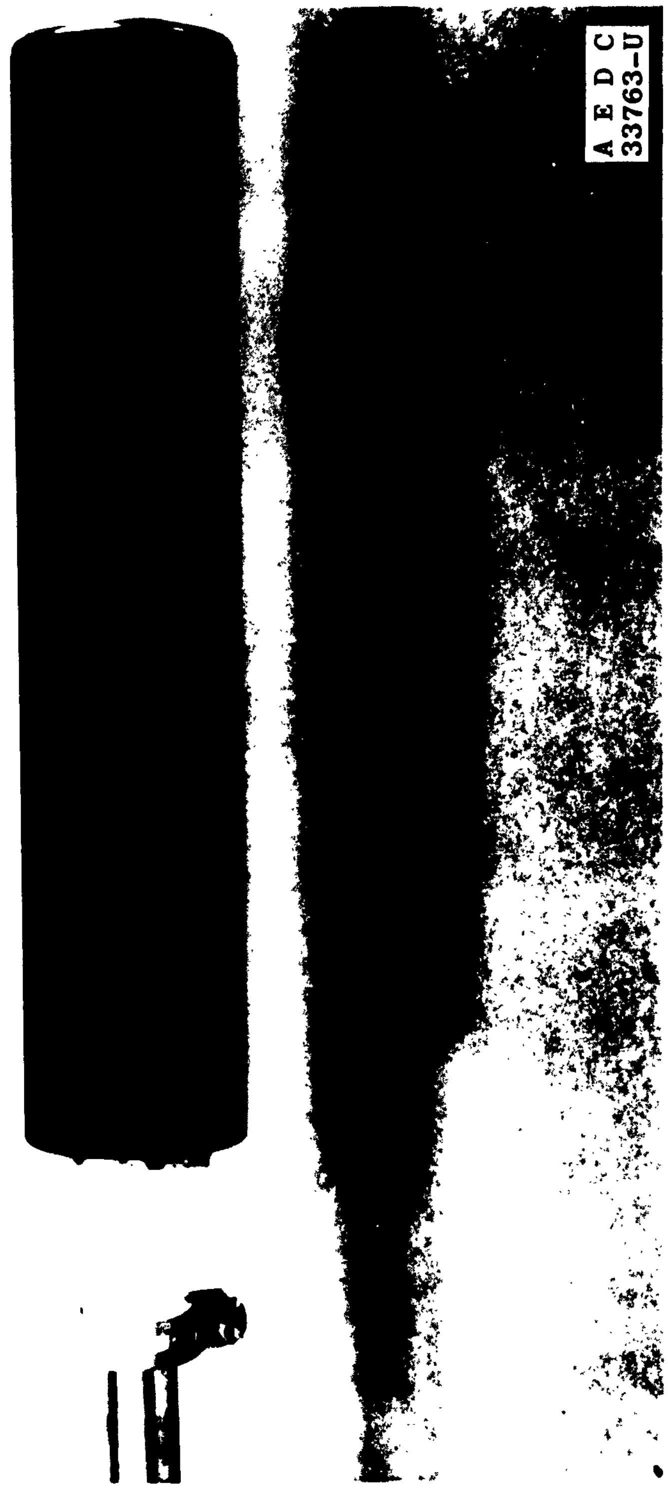

Fig. 3 Blackbody Heater

Fig. 4 Evaporated Aluminum Test Surface

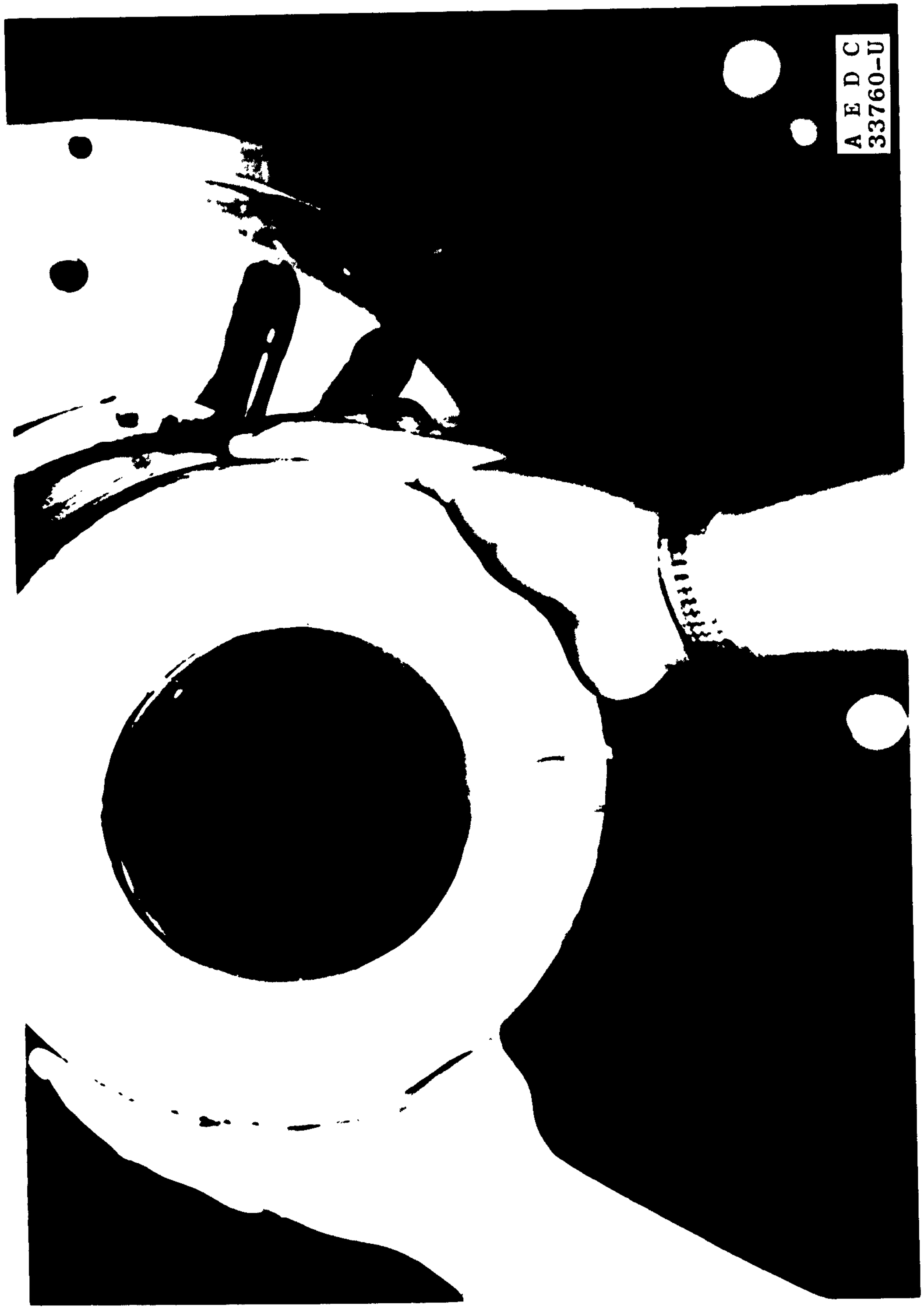

Fig. 5 Parson's Black Test Surface

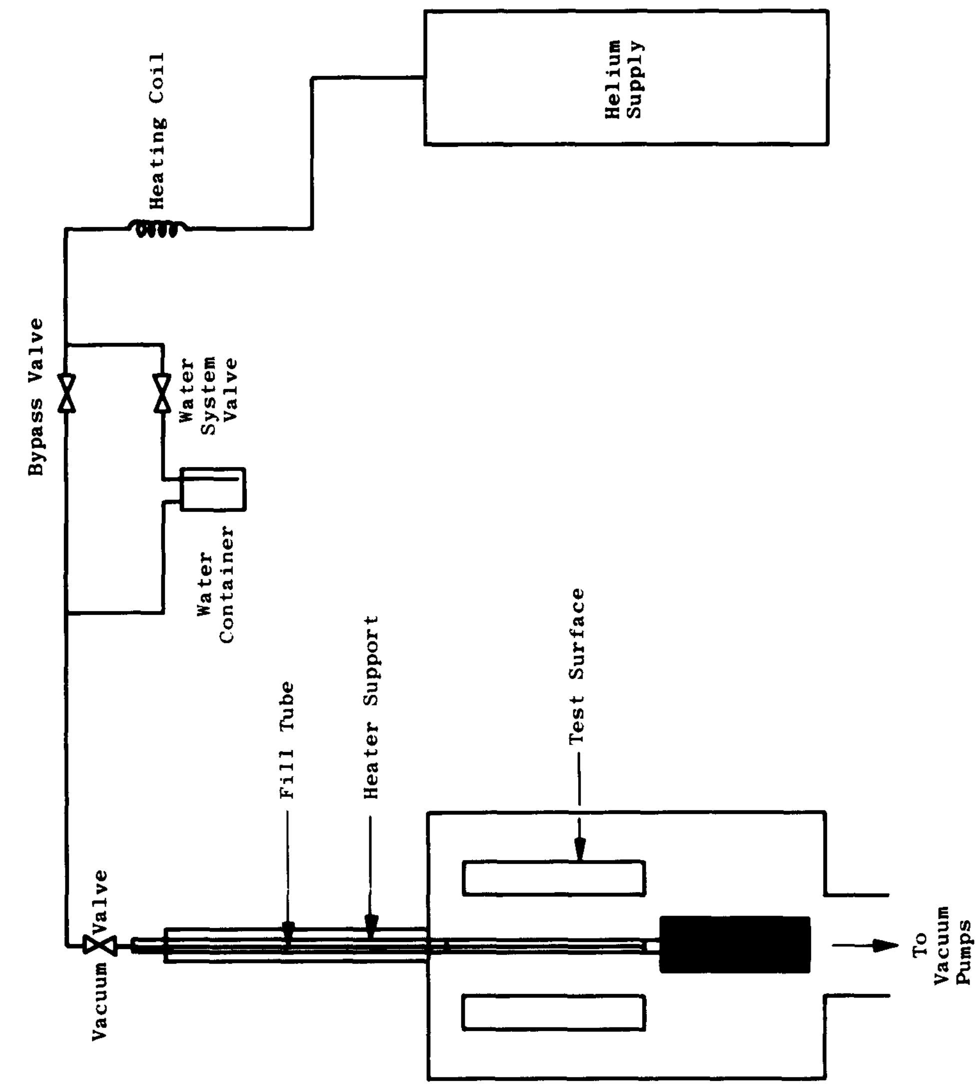

Fig. 6 Schematic of Gas Injection System

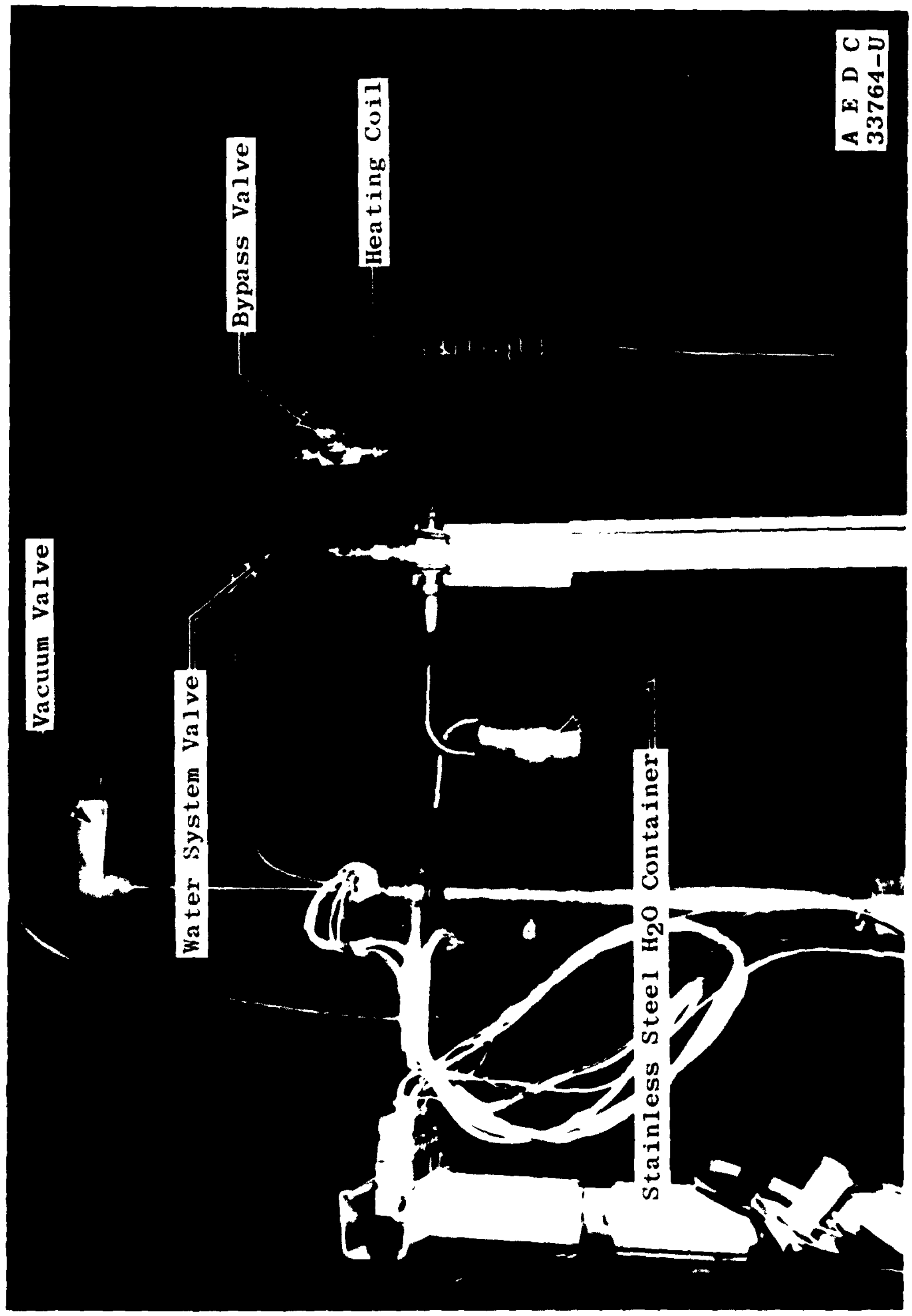

Fig. 7 Gas Injection System

Fig. 8 Gas Injection Holes in Heater Support

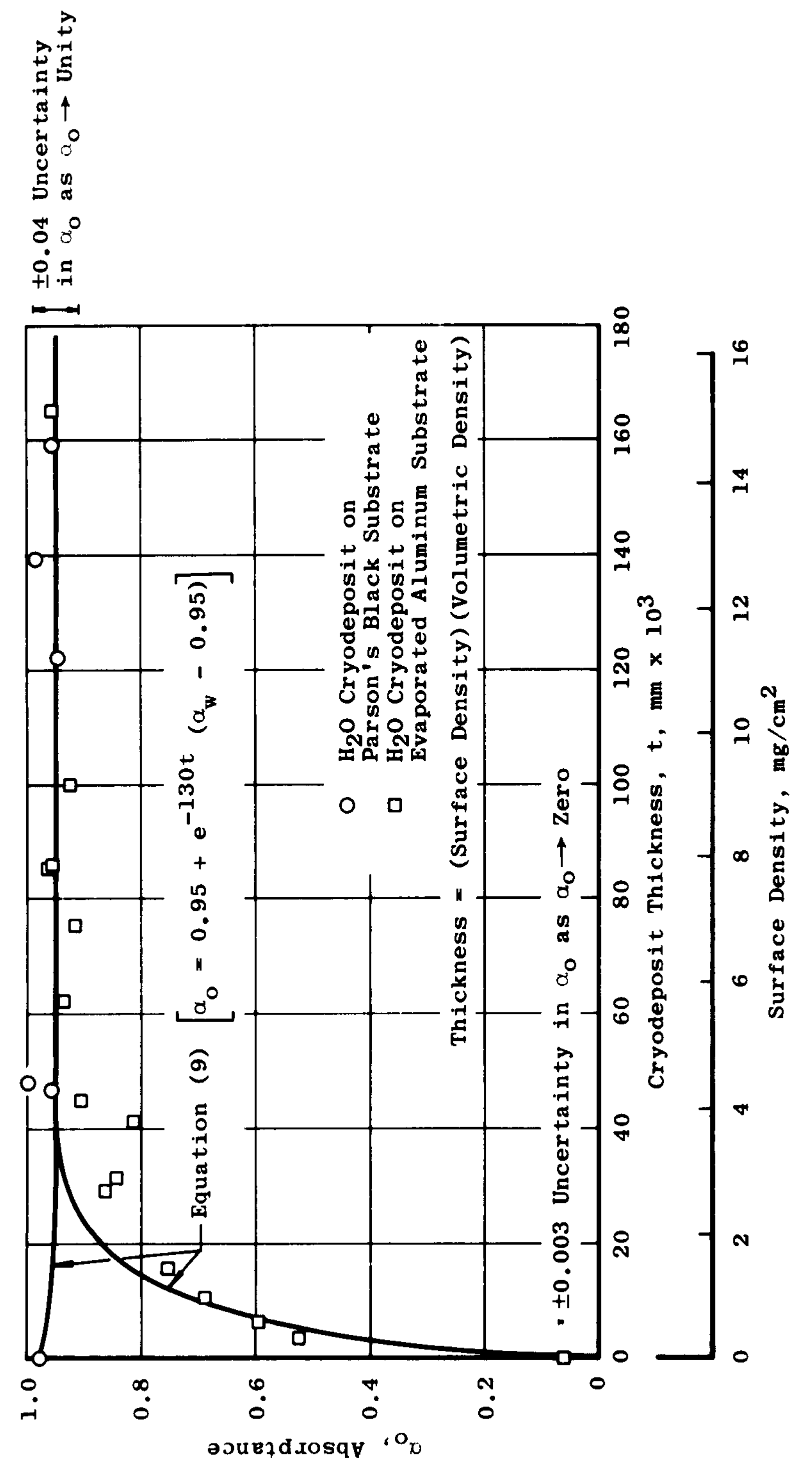

Fig. 9 Absorptance of a Water Cryodeposit